ATP release and P_2Y receptor signalling are essential for keratinocyte galvanotaxis

Aimie Riding and Christine E. Pullar*

Department of Cell Physiology and Pharmacology, University of Leicester, Leicester. U.K.

* Corresponding author: University of Leicester, Department of Cell Physiology & Pharmacology, PO Box 138, University Rd, Leicester LE1 9HN, U.K. Tel: +44 116 229 7139 Fax: +44 116 252 5045

cp161@le.ac.uk

Running title: Role of ATP in keratinocyte galvanotaxis

Key words

- Keratinocyte migration
- Directional migration
- Galvanotaxis
- Electrotaxis
- Hemi channels

Contract grant sponsor: Wellcome Trust; contract grant number: 82586.

6 Figures (1 colour: Figure 3)

Abstract

Repair to damaged tissue requires directional cell migration to heal the wound. Immediately upon wounding an electrical guidance cue is created with the cathode of the electric field (EF) located at the center of the wound. Previous research has demonstrated directional migration of keratinocytes towards the cathode when an EF of physiological strength (100-150mV/mm) is applied *in vitro*, but the "sensor" by which keratinocytes sense the EF remains elusive.

Here we use a customised chamber design to facilitate the application of a direct current (DC) EF of physiological strength (100 mV/mm) to keratinocytes whilst pharmacologically modulating the activation of both connexin hemichannels and purinergic receptors to determine their role in EF-mediated directional keratinocyte migration, galvanotaxis. In addition, keratinocytes were exposed to $DiSBAC_2(3)$ dye to visualize membrane potential changes within the cell upon exposure to the applied DC EF.

Here we unveil ATP-medicated mechanisms that underpin the initiation of keratinocyte galvanotaxis. The application of a DC EF of 100 mV/mm releases ATP via hemichannels activating a subset of purinergic P_2Y receptors, locally, to initiate the directional migration of keratinocytes towards the cathode *in vitro*, the center of the wound *in vivo*. The delineation of the mechanisms underpinning galvanotaxis extends our understanding of this endogenous cue and will facilitate the optimization and wider use of EF devices for chronic wound treatment.

Introduction

Repair to damaged tissue requires directional cell migration to heal the wound and it is essential to repair the epidermis quickly to reduce the risk of infection and restore epidermal barrier function. Wound-edge keratinocytes adopt a migratory morphology within an hour of injury, but the earliest signals responsible for initiating their migration into the wound, to commence re-epithelialisation, are unknown. Upon wounding, an electrical wound guidance cue is generated immediately, with the cathode of the electric field (EF) located at the centre of the wound. This physiological, electrical signal can be measured in acute skin wounds and is generally between 100-150mV/mm, but is reduced by 50% in elderly patients (Nuccitelli et al., 2011).

The role of direct current (DC) electric fields (EFs), both endogenous and externally applied, in biological systems such as development, tissue regeneration and cancer has attracted considerable attention in recent years (Pullar, 2011b). In the field of tissue regeneration, the complex orchestration of a number of physiological process, including keratinocyte migration and re-epithelialization, is required to repair a wound quickly, with little regard to the quality of the repaired skin (Shaw and Martin, 2009). Unfortunately, a plethora of factors can interrupt the healing process including chronic disease, vascular insufficiency, diabetes, nutritional deficiencies, infection, sustained inflammation, advanced age, mechanical pressure and neuropathies, to name a few (Fonder et al., 2008). A chronic wound is defined as a break in the skin for a long duration (> 6 weeks). They are extremely prevalent in the elderly and are both painful and debilitating for the patient and very costly. Global wound care expenditures are around 13 to 15 billion annually (Walmsley, 2002). Efforts to develop new therapies to heal chronic wounds are hampered by the lack of knowledge of both the mechanisms that drive wound healing and those responsible for the chronicity of the wounds (Stojadinovic et al., 2005). However, impaired healing coincides with alterations in keratinocyte function at the edges of chronic wounds (Stojadinovic et al., 2005; Stojadinovic et al., 2008).

Since the mid-1960's considerable research has been directed at evaluating the effects of exogenous electrical currents on the healing of chronic wounds that are frequently unresponsive to standard treatment (McCulloch, 2010). The exogenous EF is thought to supplement the endogenous electric field, generated immediately upon wounding. The endogenous EF is created due to the collapse of the trans epidermal potential (TEP) (Nuccitelli, 2003). In unwounded skin, the asymmetric distribution of ion channels in each keratinocyte layer of the multilayered epithelium generates a trans epithelial ion flow and, therefore, a voltage difference across the epidermis that is referred to as the trans epidermal potential (TEP) (Nuccitelli, 2003). A wound collapses the TEP creating a low resistance pathway for ions to flow through, returning back under the stratum corneum, to generate a lateral EF around the wound site, with the wound becoming the cathode of the endogenous EF (Nuccitelli, 2003). The existence of wound-induced DC EFs has been demonstrated experimentally in bovine cornea, human skin and other multi-layered epithelia (McCaig et al., 2005). Recently, the Bioelectric Field Imager has been used to map EFs of 100-150mV/M near linear full thickness wounds in mammalian skin (Nuccitelli et al., 2008).

Electrical stimulation (ES) has been shown in numerous clinical studies to enhance chronic wound healing (Kloth, 2005) and is now a mainstream healthcare option for persistent, non-closing wounds in the US, and has the highest level of evidence for healing chronic wounds in Europe, as described in the 2009 EPUAP guidelines (guidelines can be downloaded from (www://www.npuap.org)).This has fueled interest in the cellular mechanisms underpinning galvanotaxis.

Over the past fifteen years a number of membrane receptors: EGFR (Fang et al., 1999); $\alpha 6\beta 4$ integrins (Pullar et al., 2006); $\beta 1$ integrins (Huang et al., 2009); ion channels: the epithelial sodium channel (ENaC) (Yang et al., 2013); ions: Ca^{2+} (Huang et al., 2009; Trollinger et al., 2002); torque on charged membrane proteins as suggested in the electromechanical transduction model (Hart et al., 2013) and cytoplasmic signaling proteins: PKA (Pullar et al., 2001); cAMP (Pullar and Isseroff, 2005); extracellular-signal-regulated

kinase (ERK); p38 mitogen-activated kinase (MAPK); Src; Akt; phosphatidylinositol 3 kinase (PI3K); (Zhao et al., 2006) have been demonstrated to form part of the downstream signaling mechanisms underpinning the keratinocyte electrical compass. However, the “sensor” by which cells initially detect the presence of an applied EF remains elusive (Nuccitelli, 2003; McCaig et al. 2005; Pullar, 2009). Here we investigate the role of ATP release and purinergic receptor activation in the ability of keratinocytes to sense and respond to an applied EF of physiological strength (100 mV/mm) *in vitro* with directional migration.

Materials and Methods

Materials

Suramin, apyrase, ATP, UDP, ADP, probenecid, and carbenoxolone disodium were purchased from Sigma-Aldrich (Poole, UK). NF157, MRS2578, MRS2179 and MRS2211 were purchased from Tocris Bioscience (Bristol, UK). Epilife and human keratinocyte growth medium (HKGS) were purchased from Cascade Biologics (Invitrogen, Paisley, UK).

Primary cell culture

Two primary human keratinocyte strains (Invitrogen), derived from neonatal foreskin epidermis, were used to generate each data set. Keratinocytes were used between passages 3 and 6. Stock cultures were maintained in an exponential growth phase, as monolayers, in plastic cell culture dishes, using Keratinocyte Growth Medium (KKGS) which consists of: Keratinocyte Basal Medium; growth supplement mix; 60 μM Calcium Chloride; 0.5% antibiotic solution (25U/ml Penicilline-25ug/ml Streptomycin, Invitrogen). The cultures were incubated at 37^{o}C in a humidified atmosphere of 5% CO_2. All treatments were tested for effects on cell viability with a trypan blue exclusion test after 4 hours of culture and no effects on cell viability were observed.

Experimental conditions

Keratinocytes were routinely plated as single cells onto collagen I-coated glass (30μg/ml, Invitrogen), in custom chambers (Pullar, 2009) for 2-6 hours prior to their placement within a heated stage (37^{o}C) upon an inverted microscope, in the presence or absence of the agent of choice and an applied EF of physiological strength (100 mV/mm), as described below (Pullar et al., 2006; Pullar and Isseroff, 2005; Pullar et al., 2001). All treatments were added at time 0, at the start of each experiment.

Galvanotaxis chambers consisted of custom made plexiglass frames to which a 45x50mm cover glass slip was attached using silicone gel (Marine grade silicone sealant, 3M), to form the bottom of the chamber. Two cover slip spacers (25x10mm) where attached to the

45x50mm cover slip to produce a channel connecting the two media reservoirs on either side of the main viewing window of the chamber. Chambers where left to dry and then soaked in water overnight to dialyze the methanol from the silicone.

After cleaning the chambers with PBS, collagen 1 was added to the central channel at a concentration of 30μg/ml and left in a humidified environment for 30 minutes before the central channel was washed twice with PBS and keratinocytes were plated onto the collagen coated channel and left for 2-3 hours to adhere. Before each experiment, a third cover slip was placed over the 2 cover slip spacers to create a closed environment of 100-105μm high over the cells, and was sealed using high vacuum grease (Dow Corning, Midland MI). The aqueducts within the media reservoirs either side then allowed media to flow freely across the chamber through the closed channel produced (Hart et al., 2013).

The electric current was applied via silver/silver chloride, coil electrodes. Agar-filled, plastic tubes served as bridges to connect the electrodes to the cell chamber. These bridges provided a long, viscous path that restricted the flow of small molecules from the electrodes into the cell chamber. Fresh agar bridges were used for each experiment. The chamber rested in a custom heated stage, which maintained the temperature of the cells at 37^{o}C. The cells were viewed through an inverted microscope objective (Pullar, 2009).

Prior to the start of each experiment, thin electrodes were briefly placed at the ends of the aqueducts while the output of the function generator was adjusted to produce the desired signal to the cells.

Images of the cells were recorded at time 0 and then every 10 minutes for one hour using an automation in Openlab software from Improvision (PerkinElmer, Coventry, UK). Cells were manually tracked and the software was used initially to calculate the true speed (μm/min) for each cell over the 60-minute period and directionality (cosine of the angle of migration (θ)) for each cell over the last 10 minutes. Values were exported to Excel to calculate the average speed and cosine values for each condition. True speed indicates the average actual distance that each cell traveled per minute over the one-hour period, rather than the

straight-line distance between the starting point and end point for each cell (net distance). The cosine (θ) describes the direction of migration and is a measure of the persistence of directionality, where θ is the angle between the field axis and the cells' path of migration during the last ten minutes of the experiment i.e. the angle between the penultimate and final cell position. The field axis is established with an angle of 0^o assigned to the cathode and an angle of 180^o assigned to the anode. A cell moving directly towards the cathode will be moving with an angle of 0^o and with therefore have a directionality of 1 (cosine (0^o) = 1). A cell moving directly towards the anode will be moving with an angle of 180^o and with therefore have a directionality of -1 (cosine (180^o) = -1). A population of cells migrating randomly will have an average cosine $(\theta) = 0$.

The response of 60-200 cells was averaged for each condition and a one-way ANOVA followed by the Dunnett's post-test was performed to determine significance; **P<0.001; *P<0.05.

Visualization of changes in membrane potential

Keratinocytes were plated into collagen-coated galvanotaxis chambers, as described above, prior to incubation for 90 minutes with 0.1µg/ml of $DiSBAC_2(3)$ dye (Dawson et al., 2006) (Molecular Probes, Invitrogen) in KGM. Cells where imaged at time 0 and then every minute for 25 minutes using an automation in Volocity software by Improvision (PerkinElmer, Coventry, UK), with shutter speed minimized to reduce photo bleaching. The excitation wavelength was 405nm and the emission wavelength was 580nm using the appropriate bandpass filters. An electric field of 100mV/mm was applied from 5 to 15 minutes. To analyze the data, regions of interest were drawn around the cells in the field of view and raw fluorescence intensity was measured within the specific regions of interest at each time point to give a relative index of membrane polarization state. An increase in fluorescence intensity indicates a relative depolarization, while a decrease indicates a relative hyperpolarization.

Results

Keratinocytes sense an EF and migrate towards the cathode of an applied electric field of 100mV/mm.

Human neonatal keratinocytes migrated randomly in the absence of an applied electric field (EF) of 100mV/mm (Figure 1A) with an average migration rate of 1.185 ± 0.056 μm/minute (Figure 1C) and an average cosine of zero (cosine = -0.038 ± 0.09) (Figure 1D). Migration was random throughout the experiment with the cosine remaining zero (Figure 1E).

In contrast, in the presence of an applied EF of 100mV/mm, keratinocytes sensed and migrated directionally towards the cathode of the applied EF (Figure 1B). While the application of the EF had no effect on the speed of migration (1.056 ± 0.06 μm/minute) (Figure 1C), there was a significant increase in the directionality of migration with an average cosine of 0.719 ± 0.06 (Figure 1D). A more detailed investigation of cell directionality throughout the one-hour experiments demonstrated that keratinocytes sensed the applied EF within the first ten minutes (cosine = 0.45 ± 0.05). The directionality of migration gradually increased during the experiment (Figure 1F). Adult keratinocytes migrate 50% slower (speed 0.5 ± 0.07 μm/minute), but with a similar average cosine of 0.65 ± 0.06 (results not shown).

Apyrase decreases keratinocyte galvanotaxis.

Keratinocytes release ATP upon media change and mild mechanical stimulation (Dixon et al., 1999) and interconvert nucleotides at the cell surface, resulting in additional ATP generation (Burrell et al., 2005). In order to determine if ATP release from keratinocytes played a role in their ability to sense an applied EF and migrate directionally, apyrase (3.2U/ml), an enzyme that catalyses the hydrolysis of ATP (Zimmermann, 2000), was applied to the keratinocytes at the same time as the EF. In the presence of apyrase, while

there was no change in migration rate (Figure 2A), the directionality of migration decreased by 51% to 0.35 ± 0.07 (Figure 2B).

To investigate the role of keratinocyte ATP release in galvanotaxis further, ATP (50μM) was added to the media at the start of the experiment, to swamp endogenous release and to mask any polarized ATP release from the cells. In the absence of applied ATP, the speed of migration gradually increased during each experiment in either the presence (Figure 2C) or the absence of an applied EF (results not shown). In the applied EF, there was no effect on keratinocyte speed within the first 10 minutes of ATP application. However, from 20 minutes through to 60 minutes, speed was reduced by 10-23% (Figure 2C) and by 22% overall (Figure 2D). In contrast, exogenous ATP addition had a significant effect on the directionality of keratinocyte migration within the first 10 minutes of the experiment. Indeed, the cells were completely unable to sense and respond to the applied EF and migrated randomly, in this initial time frame (cosine = -0.05 ± 0.04) (Figure 2E). ATP is rapidly hydrolyzed (Zimmermann, 2000), therefore, it is not surprising that the inhibitory effect of exogenous ATP on keratinocyte galvanotaxis gradually reduced over time. The directionality of keratinocyte migration decreased by 66% after 20 minutes, 59% after 30 minutes, 30% after 40 minutes, 21% after 50 minutes and 25% after 60 minutes (Figure 2E).

Application of hemichannel blockers reduces the ability of keratinocytes to sense and respond to an EF.

While keratinocytes readily release ATP, as described above, the mechanism for this release is unknown (Burrell et al., 2005). Nucleotides can be released through hemichannels (Evans et al., 2006), formed from connexin (Cx) (Dbouk et al., 2009) or pannexin (Px) subunits (Barbe et al., 2006; Schenk et al., 2008), that can be opened via a variety of mechanisms including lowering extracellular calcium concentrations, mechanical stress and membrane depolarization (Evans et al., 2006). The expression of a number of Connexins (Cx) (Cx26, Cx30, Cx30.3, Cx31, Cx32, Cx43 and Cx45) (Di et al., 2001) and pannexins (Px)

(Px1 (Celetti et al., 2010) and Px3 (Bruzzone et al., 2003)) has been confirmed in human skin.

To explore the role of Cx and Px in keratinocyte galvanotaxis, experiments were performed in the presence of carbenoxolone disodium (Cbx, 100μM), which blocks both Cx and Px hemichannels (Ma et al., 2009; Sagar and Larson, 2006). Cbx increased the speed of migration by 54% to 1.624 ± 0.07 μm/minute (Figure 3A). In contrast, directional migration was abolished and the cells migrated randomly with a cosine of zero (0.099± 0.13), (Figure 3B).

To specifically examine the role of Px in keratinocyte galvanotaxis, a lower concentration of Cbx (1μM) was used, as Px are 5-20 fold more sensitive to inhibition by Cbx than Cx (Ma et al., 2009). While the keratinocyte migration rate increased by 28% (Figure 3A), directionality was decreased by 39% (Figure 3B). To further explore the role of Px in keratinocyte galvanotaxis, a second Px inhibitor, probenecid (10μM) (Silverman et al., 2008), was used. Probenecid also increased keratinocyte speed by 28% (Figure 3A), while directionality was decreased by 61% (Figure 3B).

The hemichannel mediated ATP release could occur in an asymmetrical fashion after application of an applied EF, establishing asymmetric intracellular signaling, facilitating the cell turning or repositioning required for keratinocyte directional migration towards the cathode. Hemichannels can be opened via a variety of mechanisms including membrane depolarization (Evans et al., 2006). The application of an EF will induce an asymmetric effect on membrane polarization, hyperpolarizing the membrane facing the anode and depolarizing the cathodal-facing membrane. Indeed, when an EF of 100 mV/mm is applied to a cell with a 20 μM radius it will hyperpolarize the membrane facing the anode by 2.5 mV and will depolarize the membrane facing the cathode by the same amount (Patel and Poo, 1982; Poo, 1981).

To visualize the EF-mediated alterations in membrane potential, we loaded keratinocytes with the membrane potential dye, $DiSBAC_2(3)$. This potential-sensitive probe can enter depolarized cells where it binds to intracellular proteins or membrane and exhibits enhanced

fluorescence and a red spectral shift. Increased membrane depolarization results in an additional influx of the anionic dye and an increase in fluorescence. Conversely, hyperpolarization is indicated by a decrease in fluorescence.

A decrease in mean fluorescence was detected within one minute of applying a 100mV/mm EF, indicating membrane hyperpolarization (Figure 3C). The drop in fluorescence continued until the EF was removed, after which mean fluorescence intensity gradually increased to return to levels observed prior to EF application (Figures 3C, D). Photo-bleaching was detected when experiments extended beyond 25 minutes (results not shown). Unfortunately, more detailed membrane potential changes at the cathode and anode-facing poles of the cell could not be determined, as magnification could not be enhanced to the required level to visualize these changes.

Application of the non-specific purinergic receptor antagonist, Suramin blocks the ability of cells to sense and respond to an applied electric field.

ATP can activate purinergic P_2 receptors to initiate intracellular signaling cascades. There are two families of P_2 receptors, ionotropic P_2X nucleotide-gated ion channels and metabotropic P_2Y G protein coupled receptors (Burnstock, 2006). There are seven P_2X receptor subtypes (P_2X_{1-7}) (Roberts et al., 2006) and human keratinocytes express P_2X_1, P_2X_3, P_2X_5 and P_2X_7 (Denda et al., 2002; Inoue et al., 2007). There are eight human subtypes of the P_2Y family (Dunn and Blakeley, 1988) and human keratinocytes express P_2Y_1, P_2Y_2, P_2Y_4, P_2Y_6, P_2Y_{11}, P_2Y_{12} and P_2Y_{13} (Inoue et al., 2005; Inoue et al., 2007; Tsukimoto M, 2010), with the P_2Y_2 receptor being functional (Burrell et al., 2003; Taboubi et al., 2007) and located in the basal layer of the epidermis in adult skin (Greig et al., 2003).

To determine the role of purinergic receptors in keratinocyte galvanotaxis, experiments were performed in the presence of the non-specific purinergic receptor antagonist suramin (Dunn and Blakeley, 1988). Migration speed was increased by 49% and 36% at 1 pM and 1 nM suramin, respectively (Figure 4A), while at 1 μM and 10 μM suramin, there was no effect on migration rate (Figure 4A). In contrast, there was no effect on directional migration in the

presence of 1pM suramin, however, at 1nM, 1μM and 10μM suramin, directionality was decreased by 61%, 60% and 87%, respectively. Indeed in the presence of 10μM suramin, cell migration was random (cosine of 0.09 ± 0.09; Figure 4B).

Application of specific P_2Y purinergic receptor modulators altered keratinocyte galvanotaxis.

Previous research has indicated roles for calcium (Huang et al., 2009; Trollinger et al., 2002), cAMP (Pullar and Isseroff, 2005), PKA (Pullar et al., 2001), Src, Akt, PI3K and ERK (Zhao et al., 2006) signaling in keratinocyte galvanotaxis. All of these downstream signaling pathways can all be activated by P_2Y receptors, members of the metabotropic G-protein coupled receptor family.

In order to determine if P_2Y receptors play a role in galvanotaxis, the nucleotide ADP was added to keratinocytes in the presence of an EF. ADP acts as a strong agonist for P_2Y_1, P_2Y_{12}, and P_2Y_{13} (Abbracchio et al., 2006) and a weaker agonist for P_2Y_6 and P_2Y_{11} (Ralevic. V, 1998), all of which have been shown to be expressed in human keratinocytes (Inoue et al., 2005; Inoue et al., 2007; Tsukimoto M, 2010). ADP (100μM) decreased migration rate by 35% (Figure 5A) and directionality of migration by 79% after 30 minutes (results not shown) and by 56% after 60 minutes (Figure 5B). As ADP is a weak agonist for P_2Y_6 and P_2Y_{11} (Ralevic. V, 1998), galvanotaxis was performed in the presence of 10μM and 1μM in an attempt to tease out the roles of these receptors. At a concentration of 10μM, ADP decreased the rate of migration by 18% (Figure 5A) and directionality of migration by 58% (Figure 5B). At 1μM, ADP had no effect on migration rate (Figure 5A) but decreased directional migration by 18% (Figure 5B).

In order to determine specific roles for P_2Y receptors targeted by ADP, experiments were performed in the presence of a number of selective antagonists, specifically for P_2Y_1 (MRS2179 (500nM) (Boyer et al., 1998)); P_2Y_{12} (ticlopidine hydrochloride (10μM) (Savi and Herbert, 2005)); and P_2Y_{13} (MRS2211 (1μM) (Kim et al., 2005)). The P_2Y_1 selective antagonist MRS2179 had no effect on directionality of migration (Figure 5D) or the migration

rate of keratinocytes (Figure 5C). In contrast, the two other antagonists altered both directionality and speed of migration. The P_2Y_{12} antagonist, ticlopidine hydrochloride, increased speed of migration by 78% (Figure 5C), whilst decreasing directionality by 26% (Figure 5D). The P_2Y_{13} specific antagonist MRS2211, showed similar results, producing a 38% increase in migration rate (Figure 5C) with a 32% decrease in directionality of migration (Figure 5D).

To specifically look at the role of P_2Y_6 and $P_2Y_{11,}$ specific agonists and antagonists were used. UDP (100μM), a specific agonist for P_2Y_6 (Abbracchio et al., 2006), had no effect on migration rate (Figure 5E) while decreasing the cosine of migration by 65% to 0.25 ± 0.08 (Figure 5F). To explore the role of P_2Y_6 in keratinocyte galvanotaxis further, experiments were conducted in the presence of the specific P_2Y_6 antagonist MRS2578. Speed of keratinocyte migration was reduced by 47% (Figure 5E), while directionality of migration was completely abolished (Figure 5F). Similar effects were seen with NF157, a potent P_2Y_{11} antagonist, which decreased migration rate by 66% (Figure 5G), and reduced the directionality of migration by 80% (Figure 5H).

Discussion

Summary

Keratinocytes sense and migrate directionally towards the cathode in an applied direct current (DC) electric field (EF) of 100mV/mm. Although many downstream signaling effectors such as: Ca2+ (Huang et al., 2009; Trollinger et al., 2002); PKA (Pullar et al., 2001); cAMP (Pullar and Isseroff, 2005); Src; Akt; phosphatidylinositol 3 kinase (PI3K) and Extracellular-signal-regulated kinase (ERK) (Zhao et al., 2006) and receptors/ion channels such as: β4 integrin; EGFR (Pullar et al., 2006) and ENaC (Yang et al., 2013) have been demonstrated to play a role in electrical sensing, the initial "sensor" by which keratinocytes are able to sense and then respond to an applied EF remains elusive. Here, we demonstrate that ATP release, connexin/pannexin hemichannels and a sub set of P_2Y receptors are essential for galvanotaxis. The use of $DiSBAC_2(3)$ dye, demonstrates that the application of a DC EF alters membrane potential which can be seen within one minute of application. Novel roles for $G\alpha q_{11}$ coupled P_2Y_6, duel $G\alpha q_{11}$/ $G\alpha s$ coupled P_2Y_{11}, and $G\alpha i$ coupled P_2Y_{12} and P_2Y_{13} in keratinocyte migration and galvanotaxis are revealed. In contrast, $G\alpha q$-coupled P_2Y_1 is not required for keratinocyte EF sensing or motility.

The importance of ATP release in wound healing and directional migration, a possible damage signal.

ATP acts as an early signal to trigger wound healing responses upon epithelial injury of a human corneal epithelial cell monolayer, including an increase in HB-EGF shedding, subsequent EGFR transactivation and its downstream signaling promoting wound healing (Yin et al., 2007). Indeed, stressful conditions, such as membrane disruption by cholesterol depletion, induce ATP release, which subsequently activates ERK signaling pathways to promote HB-EGF synthesis and secretion from keratinocytes (Giltaire et al., 2011).

In addition, the mechanosensitive release of ATP from hemichannels accelerates wound closure in scratch-wounded keratinocytes. The diffusion of released ATP causes intracellular

Ca2+ waves that are propagated towards rear cells in the cell sheet in a P_2Y-dependent manner (Takada et al., 2014). As keratinocytes migrate collectively as a sheet/tongue during wound healing (Eming et al., 2014) it is likely that similar processes occur *in vivo*. Indeed, ATP release from tail fin wounds drives basal epithelial cell motility in zebrafish tail fin wounds (Gault et al., 2014).

Research described herein supports a role for ATP release, hemichannels and downstream purinergic receptor signaling in the initial sensing of the applied EF and subsequent keratinocyte galvanotaxis. Indeed, a role for ATP in chemotaxis, directional migration in a chemical gradient, has been described. ATP is released from the leading edge of the neutrophil, amplifying chemotactic signals, orienting the cell via P_2Y_2 receptors and through its hydrolysis to adenosine via the ecto-nucleoside CD39 (Corriden et al., 2008), promoting cell migration via A3 adenosine receptors (Chen et al., 2006).

The importance of ATP in keratinocyte galvanotaxis is underpinned by the loss of directionality in the presence of Apyrase, which breaks down ATP, resulting in random migration within an applied EF (Figure 2). Similar results were observed upon the application of extracellular ATP, masking ATP release from the keratinocytes and suggesting that EF-mediated ATP release could be asymmetric and polarised. Our current hypothesis is that, as in neutrophil chemotaxis (Corriden et al., 2008), ATP is released from hemichannels at one edge of the cell and acts in a localized manner on a P_2Y receptor subset to allow the cell to sense the applied EF and migrate towards the cathode.

How does the EF lead to ATP release and through what mechanism is ATP released from the cell?

The mechanism through which ATP is released from keratinocytes is currently unknown, however ATP is released from cardiac fibroblasts through connexin/pannexin hemichannels, which activates P_2Y_2 receptors increasing ERK phosphorylation, alpha smooth muscle α actin expression and collagen accumulation (Lu et al., 2012).

EF-Directed keratinocyte migration was both Cbx and Probenecid sensitive, suggesting that hemichannels consisting of both connexin and pannexin subunits are the likely route through which ATP is released in keratinocyte galvanotaxis (Figure 3A, B).

The question remains as to what triggers hemichannel opening, allowing subsequent ATP release. As applied EFs alter membrane potential, depolarizing the membrane facing the cathode (Patel and Poo, 1982; Poo, 1981) and as hemichannels can open upon membrane depolarization (Evans et al., 2006), we hypothesize that depolarization occurs at the cathodal-facing keratinocyte plasma membrane, upon EF application, opening hemichannels and releasing ATP. Recently changes in membrane polarization have been shown to play a role in Dictyostelium galvanotaxis (Gao et al., 2011).

The visualization of membrane potential changes, in keratinocytes exposed to an applied EF, was through the use of $DiSBAC_2$ dye. The results suggest that hyperpolarization occurs within the first minute of EF exposure, represented by a decrease in fluorescence (Figure 3C, D). Attempts to visualize localized membrane potential changes at the cathodal facing side of the cell failed due to limitations in magnification. Earlier attempts to visualize EF-mediated alterations in membrane potential have demonstrated that, in an large EF of 53 V/cm, cancer cells appeared hyperpolarized facing the anode and depolarized facing the cathode (Gross et al., 1986). This is in contrast however to recent evidence in primary rat osteoblasts (calvaria; migrate cathodally) and human osteosarcoma cells (SaOS-2; migrate anodally) which were exposed to hyper-physiological EFs of 5 V/cm and surprisingly, the membrane facing the direction of migration appeared hyperpolarized (Ozkucur et al., 2009) rather than depolarized. The exact localized changes in membrane potential and, therefore, polarization state, at each pole of the cell, upon keratinocyte exposure to an applied EF, are currently unknown.

It is interesting to note, however, that a number of ions, ion channels and charge involvement have already been described as playing a role in keratinocyte EF sensing: the epithelial sodium channel (ENaC) (Yang et al., 2013); ions: Ca^{2+} (Huang et al., 2009; Trollinger et al., 2002) and torque on charged membrane proteins, as suggested in the

electromechanical transduction model (Hart et al., 2013). Naturally, any change in membrane potential requires ion movement, generally potassium ion efflux at one pole to generate a hyperpolarized membrane potential with an equal level of depolarization at the opposite pole. The theory described herein fits perfectly with previously published work demonstrating the involvement of potassium ion channels in keratinocyte galvanotaxis. A 50% decrease in EF-mediated directionality was observed in the presence of potassium channel blockers 4-AP (500μM) and TEA (500μM) with no effect on the speed of keratinocyte migration (Pullar, 2011a).

How does ATP activate intracellular signaling cascades to initiate directional migration? A role for Purinergic receptors.

ATP plays an important role in neutrophil chemotaxis via the metabotropic purinergic P_2Y_2 receptor (Chen et al., 2006), and microglial chemotaxis via P_2Y_{12} (Honda et al., 2001; Irino et al., 2008; Ohsawa et al., 2007) and P_2X_4 (Ohsawa et al., 2007) a ligand gated ion channel. Here we show the non-specific purinergic receptor antagonist suramin, targeting both P_2Y and P_2X receptors, completely blocked the cells ability to sense and respond to the applied EF (Figure 4), strongly suggesting a role for purinergic receptors and their downstream signaling cascades in keratinocyte galvanotaxis.

The ATP-mediated activation of purinergic receptors can directly activate the majority of the downstream signaling proteins currently identified as playing a role in galvanotaxis including increases in intracellular Ca^{2+}(Huang et al., 2009; Trollinger et al., 2002) and activation of a number of cytoplasmic signaling proteins including: PKA (Pullar et al., 2001); cAMP (Pullar and Isseroff, 2005); Src; Akt; phosphatidylinositol 3 kinase-γ (PI3Kγ) and Extracellular-signal-regulated kinase (ERK) (Zhao et al., 2006). The $G\alpha q_{11}$-coupled P_2YR (P_2Y_1, P_2Y_2, P_2Y_4, P_2Y_6,) activate PLC, cleaving PIP_2 and leading to IP3-mediated calcium release; the Gαi-coupled purinergic receptors (P_2Y_{12}, P_2Y_{13}) couple to PI3Kγ, Akt, cAMP and src, and the duel Gαs/ $G\alpha q_{11}$ coupled P_2Y_{11}, activates either cAMP and PKA, or IP3-medicated calcium

release (Burnstock, 2006). It is, therefore, not surprising that keratinocyte galvanotaxis was compromised by either agonists or antagonists of P_2Y_6, P_2Y_{11}, P_2Y_{12} and P_2Y_{13} (Figure 5). However, a specific antagonist of P_2Y_1, MRS2179, had not effect on keratinocyte migration or directional migration (Figure 5C, D).

Experiments with ADP demonstrate that a subset of receptors: $G\alpha q_{11}$ coupled P_2Y_6; duel $G\alpha q_{11}$/ $G\alpha s$ coupled P_2Y_{11} and $G\alpha i$ coupled P_2Y_{12} and P_2Y_{13} could play a role in both keratinocyte motility and galvanotaxis, while $G\alpha q$-coupled P_2Y_1 was not required for keratinocyte EF sensing or motility. Experiments performed with the P_2Y_{12} antagonist ticlopidine hydrochloride and MRS2211, a P_2Y_{13} antagonist, revealed a similar effect on keratinocyte motility and galvanotaxis, an increase in motility and a decrease in galvanotaxis. In order to respond to a directional cue, cells must halt or slow migration to physically turn or re-arrange their intracellular compass signaling machinery to begin to migrate directionally. It makes sense, therefore, that if you block a receptor that plays a role in directional sensing that you would see a decrease in directional migration but also an increase in migration speed as seen for both P_2Y_{12} and P_2Y_{13}. It is highly likely, therefore that $G\alpha i$ coupled P_2Y_{12} and P_2Y_{13} are directly involved in keratinocyte galvanotaxis. This is supported by previously published work, which demonstrates that directional migration is a cAMP dependent process, whilst keratinocyte migration is a cAMP independent process (Pullar and Isseroff, 2005). Activation of $G\alpha i$ lowers cAMP generation from adenylyl cyclase, therefore the polarized ATP-mediated activation of P_2Y_{12} and P_2Y_{13} lowering cAMP in a spatially restricted manner, facilitates keratinocyte galvanotaxis.

In contrast, antagonists to the $G\alpha q_{11}$ coupled P_2Y_6 and the duel $G\alpha q_{11}$/ $G\alpha s$ coupled P_2Y_{11} reduces both migration speed and directional migration, suggesting an involvement in both physiological processes. There is a vast amount of evidence to support the role of calcium in keratinocyte galvanotaxis and both P_2Y_6 and P_2Y_{11} couple to $G\alpha q_{11}$ which acts to increase intracellular calcium, however previous research provides a role for extracellular calcium, rather than intracellular store release (Huang et al., 2009) acting on the cells through an ion

channel mediated influx (Trollinger et al., 2002). It is possible that calcium influx occurs through the opening of L-type calcium channels upon application of an EF. Indeed, increases in intracellular calcium were mediated, in part, by these channels upon application of 200mV/mm EF's to keratinocytes (Dube.J, 2011). Both $G\alpha q_{11}$ coupled P_2Y_6 and P_2Y_{11} can induce the IP_3–mediated release of calcium from intracellular calcium stores. In fish keratinocytes, extracellular calcium influx occurs upon EF application along with intracellular calcium release which acts to set up a continuous calcium wave within the cell (Brust-Mascher and Webb, 1998). Therefore, ATP activation of P_2Y_6 and P_2Y_{11} could generate this continuous calcium wave to maintain sensing of the EF and allow directional migration towards the cathode. In addition, purinergic receptors, are also known to play a role in epithelial cell motility (Klepeis et al., 2004; Taboubi et al., 2007) and migration in other cell types (Bagchi et al., 2005; Shen and DiCorleto, 2008), while an ATP-mediated, intracellular store-dependent, increase in intracellular calcium played a role in HaCaT migration and proliferation (Lee et al., 2001).

In conclusion, an applied EF opens connexin/pannexin hemichannels releasing ATP in a polarized manner. ATP activates a subset of metabotropic P_2Y receptors locally, initiating signaling cascades known to play a role in keratinocyte galvanotaxis: calcium, cAMP and PI3Kγ (Figure 6).

Acknowledgements

The authors would like to thank Professor Richard Evans for help and advise in the field of purinergic receptor signaling and Professors Mike Levin and Dany Adams for providing the initial $DiBAC_2(3)$ dye and advice.

References:

Abbracchio, M.P., G. Burnstock, J.M. Boeynaems, E.A. Barnard, J.L. Boyer, C. Kennedy, G.E. Knight, M. Fumagalli, C. Gachet, K.A. Jacobson, and G.A. Weisman. 2006. International Union of Pharmacology LVIII: update on the P2Y G protein-coupled nucleotide receptors: from molecular mechanisms and pathophysiology to therapy. *Pharmacol Rev*. 58:281-341.

Bagchi, S., Z. Liao, F.A. Gonzalez, N.E. Chorna, C.I. Seye, G.A. Weisman, and L. Erb. 2005. The P2Y2 nucleotide receptor interacts with alphav integrins to activate Go and induce cell migration. *J Biol Chem*. 280:39050-39057.

Barbe, M.T., H. Monyer, and R. Bruzzone. 2006. Cell-cell communication beyond connexins: the pannexin channels. *Physiology (Bethesda)*. 21:103-114.

Boyer, J.L., A. Mohanram, E. Camaioni, K.A. Jacobson, and T.K. Harden. 1998. Competitive and selective antagonism of P2Y1 receptors by N6-methyl 2'-deoxyadenosine 3',5'-bisphosphate. *British journal of pharmacology*. 124:1-3.

Brust-Mascher, I., and W.W. Webb. 1998. Calcium waves induced by large voltage pulses in fish keratocytes. *Biophys J*. 75:1669-1678.

Bruzzone, R., S.G. Hormuzdi, M.T. Barbe, A. Herb, and H. Monyer. 2003. Pannexins, a family of gap junction proteins expressed in brain. *Proc Natl Acad Sci U S A*. 100:13644-13649.

Burnstock, G. 2006. Purinergic signalling. *Br J Pharmacol*. 147 Suppl 1:S172-181.

Burrell, H.E., W.B. Bowler, J.A. Gallagher, and G.R. Sharpe. 2003. Human keratinocytes express multiple P2Y-receptors: evidence for functional P2Y1, P2Y2, and P2Y4 receptors. *J Invest Dermatol*. 120:440-447.

Burrell, H.E., B. Wlodarski, B.J. Foster, K.A. Buckley, G.R. Sharpe, J.M. Quayle, A.W. Simpson, and J.A. Gallagher. 2005. Human keratinocytes release ATP and utilize three mechanisms for nucleotide interconversion at the cell surface. *J Biol Chem*. 280:29667-29676.

Celetti, S.J., K.N. Cowan, S. Penuela, Q. Shao, J. Churko, and D.W. Laird. 2010. Implications of pannexin 1 and pannexin 3 for keratinocyte differentiation. *J Cell Sci*. 123:1363-1372.

Chen, Y., R. Corriden, Y. Inoue, L. Yip, N. Hashiguchi, A. Zinkernagel, V. Nizet, P.A. Insel, and W.G. Junger. 2006. ATP release guides neutrophil chemotaxis via P2Y2 and A3 receptors. *Science*. 314:1792-1795.

Corriden, R., Y. Chen, Y. Inoue, G. Beldi, S.C. Robson, P.A. Insel, and W.G. Junger. 2008. Ecto-nucleoside triphosphate diphosphohydrolase 1 (E-NTPDase1/CD39) regulates neutrophil chemotaxis by hydrolyzing released ATP to adenosine. *J Biol Chem*. 283:28480-28486.

Dawson, N.S., D.C. Zawieja, M.H. Wu, and H.J. Granger. 2006. Signaling pathways mediating VEGF165-induced calcium transients and membrane depolarization in human endothelial cells. *Faseb J*. 20:991-993.

Dbouk, H.A., R.M. Mroue, M.E. El-Sabban, and R.S. Talhouk. 2009. Connexins: a myriad of functions extending beyond assembly of gap junction channels. *Cell Commun Signal*. 7:4.

Denda, M., K. Inoue, S. Fuziwara, and S. Denda. 2002. P2X purinergic receptor antagonist accelerates skin barrier repair and prevents epidermal hyperplasia induced by skin barrier disruption. *J Invest Dermatol*. 119:1034-1040.

Di, W.L., E.L. Rugg, I.M. Leigh, and D.P. Kelsell. 2001. Multiple epidermal connexins are expressed in different keratinocyte subpopulations including connexin 31. *J Invest Dermatol*. 117:958-964.

Dixon, C.J., W.B. Bowler, A. Littlewood-Evans, J.P. Dillon, G. Bilbe, G.R. Sharpe, and J.A. Gallagher. 1999. Regulation of epidermal homeostasis through P2Y2 receptors. *Br J Pharmacol*. 127:1680-1686.

Dube.J, Rochette-Drouin.O., Levesque.P, Gauvin.R, Roberge.CJ, Auger.FA, Goulet.D, Bourdages.M, Plante.M, Moulin.VJ, Germain.L. 2011. Human Keratinocyres Responde to Direct Current Stimulation by Increasing Intracellular Calcium: Preferential Response of Poorly Differenciated Cells. *J Cell Physiol*: 227:2660-2667.

Dunn, P.M., and A.G. Blakeley. 1988. Suramin: a reversible P2-purinoceptor antagonist in the mouse vas deferens. *British journal of pharmacology*. 93:243-245.

Eming, S.A., P. Martin, and M. Tomic-Canic. 2014. Wound repair and regeneration: mechanisms, signaling, and translation. *Science translational medicine*. 6:265sr266.

Evans, W.H., E. De Vuyst, and L. Leybaert. 2006. The gap junction cellular internet: connexin hemichannels enter the signalling limelight. *Biochem J*. 397:1-14.

Fang, K.S., E. Ionides, G. Oster, R. Nuccitelli, and R.R. Isseroff. 1999. Epidermal growth factor receptor relocalization and kinase activity are necessary for directional migration of keratinocytes in DC electric fields. *J Cell Sci*. 112:1967-1978.

Fonder, M.A., G.S. Lazarus, D.A. Cowan, B. Aronson-Cook, A.R. Kohli, and A.J. Mamelak. 2008. Treating the chronic wound: A practical approach to the care of nonhealing wounds and wound care dressings. *Journal of the American Academy of Dermatology*. 58:185-206.

Gao, R.C., X.D. Zhang, Y.H. Sun, Y. Kamimura, A. Mogilner, P.N. Devreotes, and M. Zhao. 2011. Different roles of membrane potentials in electrotaxis and chemotaxis of dictyostelium cells. *Eukaryot Cell*. 10:1251-1256.

Gault, W.J., B. Enyedi, and P. Niethammer. 2014. Osmotic surveillance mediates rapid wound closure through nucleotide release. *J Cell Biol*. 207:767-782.

Giltaire, S., S. Lambert, and Y. Poumay. 2011. HB-EGF synthesis and release induced by cholesterol depletion of human epidermal keratinocytes is controlled by extracellular ATP and involves both p38 and ERK1/2 signaling pathways. *Journal of cellular physiology*. 226:1651-1659.

Greig, A.V., C. Linge, G. Terenghi, D.A. McGrouther, and G. Burnstock. 2003. Purinergic receptors are part of a functional signaling system for proliferation and differentiation of human epidermal keratinocytes. *J Invest Dermatol*. 120:1007-1015.

Gross, D., L.M. Loew, and W.W. Webb. 1986. Optical imaging of cell membrane potential changes induced by applied electric fields. *Biophysical Journal*. 50:339-348.

Hart, F.X., M. Laird, A. Riding, and C.E. Pullar. 2013. Keratinocyte galvanotaxis in combined DC and AC electric fields supports an electromechanical transduction sensing mechanism. *Bioelectromagnetics*. 34:85-94.

Honda, S., Y. Sasaki, K. Ohsawa, Y. Imai, Y. Nakamura, K. Inoue, and S. Kohsaka. 2001. Extracellular ATP or ADP induce chemotaxis of cultured microglia through Gi/o-coupled P2Y receptors. *J Neurosci*. 21:1975-1982.

Huang, L., P. Cormie, M.A. Messerli, and K.R. Robinson. 2009. The involvement of Ca2+ and integrins in directional responses of zebrafish keratocytes to electric fields. *J Cell Physiol*. 219:162-172.

Inoue, K., M. Denda, H. Tozaki, K. Fujishita, S. Koizumi, and K. Inoue. 2005. Characterization of multiple P2X receptors in cultured normal human epidermal keratinocytes. *J Invest Dermatol*. 124:756-763.

Inoue, K., J. Hosoi, and M. Denda. 2007. Extracellular ATP has stimulatory effects on the expression and release of IL-6 via purinergic receptors in normal human epidermal keratinocytes. *J Invest Dermatol*. 127:362-371.

Irino, Y., Y. Nakamura, K. Inoue, S. Kohsaka, and K. Ohsawa. 2008. Akt activation is involved in P2Y12 receptor-mediated chemotaxis of microglia. *J Neurosci Res*. 86:1511-1519.

Kim, Y.C., J.S. Lee, K. Sak, F. Marteau, L. Mamedova, J.M. Boeynaems, and K.A. Jacobson. 2005. Synthesis of pyridoxal phosphate derivatives with antagonist activity at the P2Y13 receptor. *Biochemical pharmacology*. 70:266-274.

Klepeis, V.E., I. Weinger, E. Kaczmarek, and V. Trinkaus-Randall. 2004. P2Y receptors play a critical role in epithelial cell communication and migration. *J Cell Biochem*. 93:1115-1133.

Kloth, L.C. 2005. Electrical stimulation for wound healing: a review of evidence from in vitro studies, animal experiments, and clinical trials. *Int J Low Extrem Wounds*. 4:23-44.

Lee, W.K., S.W. Choi, H.R. Lee, E.J. Lee, K.H. Lee, and H.O. Kim. 2001. Purinoceptor-mediated calcium mobilization and proliferation in HaCaT keratinocytes. *J Dermatol Sci*. 25:97-105.

Lu, D., S. Soleymani, R. Madakshire, and P.A. Insel. 2012. ATP released from cardiac fibroblasts via connexin hemichannels activates profibrotic P2Y2 receptors. *FASEB journal : official publication of the Federation of American Societies for Experimental Biology*. 26:2580-2591.

Ma, W., H. Hui, P. Pelegrin, and A. Surprenant. 2009. Pharmacological characterization of pannexin-1 currents expressed in mammalian cells. *The Journal of pharmacology and experimental therapeutics*. 328:409-418.

McCaig, C.D., A.M. Rajnicek, B. Song, and M. Zhao. 2005. Controlling cell behavior electrically: current views and future potential. *Physiol Rev*. 85:943-978.

McCulloch, J.M and Kloth, L. 2010. Wound Healing: Evidence-based management. F. A Davis and Company publishers, Philadelphia.

Nuccitelli, R. 2003. Endogenous electric fields in embryos during development, regeneration and wound healing. *Radiat Prot Dosimetry*. 106:375-383.

Nuccitelli, R., P. Nuccitelli, C. Li, S. Narsing, D.M. Pariser, and K. Lui. 2011. The electric field near human skin wounds declines with age and provides a noninvasive indicator of wound healing. *Wound Repair Regen*. 19:645-655.

Nuccitelli, R., P. Nuccitelli, S. Ramlatchan, R. Sanger, and P.J. Smith. 2008. Imaging the electric field associated with mouse and human skin wounds. *Wound Repair Regen*. 16:432-441.

Ohsawa, K., Y. Irino, Y. Nakamura, C. Akazawa, K. Inoue, and S. Kohsaka. 2007. Involvement of P2X4 and P2Y12 receptors in ATP-induced microglial chemotaxis. *Glia*. 55:604-616.

Ozkucur, N., T.K. Monsees, S. Perike, H.Q. Do, and R.H. Funk. 2009. Local calcium elevation and cell elongation initiate guided motility in electrically stimulated osteoblast-like cells. *PLoS One*. 4:e6131.

Patel, N., and M.M. Poo. 1982. Orientation of neurite growth by extracellular electric fields. *J Neurosci*. 2:483-496.

Poo, M. 1981. In situ electrophoresis of membrane components. *Annu Rev Biophys Bioeng*. 10:245-276.

Pullar, C.E. 2009. The biological basis for electric stimulation as a therapy to heal chronic wounds. *Journal of Wound Technology*. 6:20-24.

Pullar, C.E. 2011a. Physiological electric fields can direct keratinocyte migration and promote healing in chronic wounds, Chapter 6 in 2011b. CRC Press, New York.
Pullar, C.E. 2011b. The physiology of bioelectricity in development, tissue regeneration and cancer. CRC Press, New York.
Pullar, C.E., B.S. Baier, Y. Kariya, A.J. Russell, B.A. Horst, M.P. Marinkovich, and R.R. Isseroff. 2006. beta4 integrin and epidermal growth factor coordinately regulate electric field-mediated directional migration via Rac1. *Mol Biol Cell*. 17:4925-4935.
Pullar, C.E., and R.R. Isseroff. 2005. Cyclic AMP mediates keratinocyte directional migration in an electric field. *J Cell Sci*. 118:2023-2034.
Pullar, C.E., R.R. Isseroff, and R. Nuccitelli. 2001. Cyclic AMP-dependent protein kinase A plays a role in the directed migration of human keratinocytes in a DC electric field. *Cell Motil Cytoskeleton*. 50:207-217.
Ralevic. V and Burnstock. G. 1998. Receptors for purines and pyrimidines. *Pharmacol Rev*. 50(3):413-492.
Roberts, J.A., C. Vial, H.R. Digby, K.C. Agboh, H. Wen, A. Atterbury-Thomas, and R.J. Evans. 2006. Molecular properties of P2X receptors. *Pflugers Arch*. 452:486-500.
Sagar, G.D., and D.M. Larson. 2006. Carbenoxolone inhibits junctional transfer and upregulates Connexin43 expression by a protein kinase A-dependent pathway. *Journal of Cellular Biochemistry*. 98:1543-1551.
Savi, P., and J.M. Herbert. 2005. Clopidogrel and ticlopidine: P2Y12 adenosine diphosphate-receptor antagonists for the prevention of atherothrombosis. *Semin Thromb Hemost*. 31:174-183.
Schenk, U., A.M. Westendorf, E. Radaelli, A. Casati, M. Ferro, M. Fumagalli, C. Verderio, J. Buer, E. Scanziani, and F. Grassi. 2008. Purinergic control of T cell activation by ATP released through pannexin-1 hemichannels. *Sci Signal*. 1:ra6.
Shaw, T.J., and P. Martin. 2009. Wound repair at a glance. *J Cell Sci*. 122:3209-3213.
Shen, J., and P.E. DiCorleto. 2008. ADP stimulates human endothelial cell migration via P2Y1 nucleotide receptor-mediated mitogen-activated protein kinase pathways. *Circ Res*. 102:448-456.
Silverman, W., S. Locovei, and G. Dahl. 2008. Probenecid, a gout remedy, inhibits pannexin 1 channels. *Am J Physiol Cell Physiol*. 295:C761-767.
Stojadinovic, O., H. Brem, C. Vouthounis, B. Lee, J. Fallon, M. Stallcup, A. Merchant, R.D. Galiano, and M. Tomic-Canic. 2005. Molecular pathogenesis of chronic wounds: the role of beta-catenin and c-myc in the inhibition of epithelialization and wound healing. *Am J Pathol*. 167:59-69.
Stojadinovic, O., I. Pastar, S. Vukelic, M.G. Mahoney, D. Brennan, A. Krzyzanowska, M. Golinko, H. Brem, and M. Tomic-Canic. 2008. Deregulation of keratinocyte differentiation and activation: a hallmark of venous ulcers. *J Cell Mol Med*. 12:2675-2690.
Taboubi, S., J. Milanini, E. Delamarre, F. Parat, F. Garrouste, G. Pommier, J. Takasaki, J.C. Hubaud, H. Kovacic, and M. Lehmann. 2007. G alpha(q/11)-coupled P2Y2 nucleotide receptor inhibits human keratinocyte spreading and migration. *Faseb J*. 21:4047-4058.
Takada, H., K. Furuya, and M. Sokabe. 2014. Mechanosensitive ATP release from hemichannels and Ca(2)(+) influx through TRPC6 accelerate wound closure in keratinocytes. *J Cell Sci*. 127:4159-4171.
Trollinger, D.R., R.R. Isseroff, and R. Nuccitelli. 2002. Calcium channel blockers inhibit galvanotaxis in human keratinocytes. *J Cell Physiol*. 193:1-9.
Tsukimoto M, H.T., Ohshima Y, Kojima S. 2010. Involvement of purinergic signaling in cellular response to gamma radiation. *Radiat Res*. 3:298-309.

Walmsley, S. 2002. Advances in wound management: executive summary. PJB Publications, London.

www://http://www.npuap.org.

Yang, H.Y., R.P. Charles, E. Hummler, D.L. Baines, and R.R. Isseroff. 2013. The epithelial sodium channel mediates the directionality of galvanotaxis in human keratinocytes. *J Cell Sci*. 126:1942-1951.

Yin, J., K. Xu, J. Zhang, A. Kumar, and F.S. Yu. 2007. Wound-induced ATP release and EGF receptor activation in epithelial cells. *J Cell Sci*. 120:815-825.

Zhao, M., B. Song, J. Pu, T. Wada, B. Reid, G. Tai, F. Wang, A. Guo, P. Walczysko, Y. Gu, T. Sasaki, A. Suzuki, J.V. Forrester, H.R. Bourne, P.N. Devreotes, C.D. McCaig, and J.M. Penninger. 2006. Electrical signals control wound healing through phosphatidylinositol-3-OH kinase-gamma and PTEN. *Nature*. 442:457-460.

Zimmermann, H. 2000. Extracellular metabolism of ATP and other nucleotides. *Naunyn-Schmiedeberg's archives of pharmacology*. 362:299-309.

Figure Legends

Figure 1: Cell migration was plotted using a circle graph with cell position at time 0 at the center of the graph (0,0). The location of the cell at the final time point at 60 minutes was plotted as a single dot in relation to directionality and distance of migration. The top of the graph represents the cathode (0) and the bottom represents the anode (180). The final position of each cell is shown in the absence (A) and presence of an applied EF of 100mV/mm^2 (B). The average speed of migration (C) and directionality of migration after 60 minutes are plotted in the absence and presence of an applied EF of 100mV/mm^2 (D) and directionality over time is presented for keratinocytes in the absence (E) and presence of an applied EF of 100mV/mm^2 (F). (Non field control n = 64; field control n = 70)** P < 0.01.

Figure 2: Cells were exposed to various treatments in the presence of an applied EF. The effect of apyrase, an enzyme that breaks down ATP, on speed of migration (A) and directionality of migration (B) is shown. A cosine of 1 represents directional migration towards the cathode, whilst a cosine of -1 represents directional migration towards the anode. A cosine of 0 represents random migration. The effect of ATP application to keratinocytes in an applied EF of 100mV/mm^2 at 60 minutes is shown (D), with a further breakdown of speed of migration at each 10-minute time point (C). The effect of ATP application on directionality is presented using cosine values at ten-minute intervals (E). (Apyrase n= 83; ATP n= 67). ** P < 0.01; *P < 0.05.

Figure 3: Pannexin/connexin hemichannel blocker carbenoxolone disodium was applied to keratinocytes in the presence of an applied EF of 100mV/mm at 100μM where connexin and pannexin channels are targeted, and at the lower concentration of 1μM where only pannexin channels are targeted. Probenecid, a pannexin specific hemichannel blocker was also applied to further demonstrate the role of pannexin hemichannels in keratinocyte

galvanotaxis. The effect of these drugs on speed of migration (A) and directionality of migration (B) is seen. Mean fluorescence intensity was measured in cells exposed to $DiSBAC_2(3)$ dye in the presence and absence of an applied EF. $DiSBAC_2(3)$ dye enters depolarized cells, binding to intracellular proteins, which leads to enhanced fluorescence. Changes in mean fluorescence intensity upon application and removal of an applied EF of 100mV/mm is presented (C) supported by images representing the changes in fluorescence seen (D). (Carbenoxolone 100μM n= 88; Carbenoxolone 1μM n= 157; Probenecid n= 249) ** $P < 0.01$

Figure 4: Suramin, a purinergic receptor antagonist, was applied to keratinocytes in an applied EF of 100mV/mm at concentrations ranging from 10^{-12}M to 10^{-5}M and the effect on speed of migration at each concentration (A) and directionality of migration (B) is shown. (10^{-5}M n= 79; 10^{-6}M n= 105; 10^{-9}M n= 111; 10^{-12}M n= 66) ** $P < 0.01$

Figure 5: ADP targets a number of purinergic receptors**.** Application of ADP at concentrations of 1μM, 10μM, and 100μM and its effect on speed of migration (A) and directionality of migration (B) are shown. The effects of specific purinergic receptor antagonists are also presented with the effect on speed of migration of MRS2179, ticlopidine hydrochloride and MRS2211 (C), UDP and MRS2578 (E) and NF157 (G) shown. The effects of these purinergic receptor blockers on directionality of migration are also separately presented; MRS2179, ticlopidine hydrochloride and MRS2211 (D), UDP and MRS2578 (F) and NF157 (H). (ADP 1μM n= 61, ADP 10μM n= 72, ADP 100μM n= 77, MRS2179 n= 45, ticlopidine hydrochloride n= 162, MRS2211 n= 172, UDP n= 61, MRS2578 n= 51, NF157 n= 59) ** $P < 0.01$; *$P < 0.05$.

Figure 6: A diagram explaining our hypothesis that application of an electric field induced polarized membrane potential changes causing hyperpolarization at one pole, likely the anode facing side, and depolarization on the opposite pole, likely the cathode facing pole of

the cell. This leads to localized ATP release through pannexin/connexin hemichannels, opened upon membrane depolarization, likely on the cathodal facing surface, in turn activating local P_2Y receptors in autocrine fashion to cause polarized activation of signaling cascades within the cell to allow directional migration towards the cathode, the center of a wound *in vivo*.

Figure 1

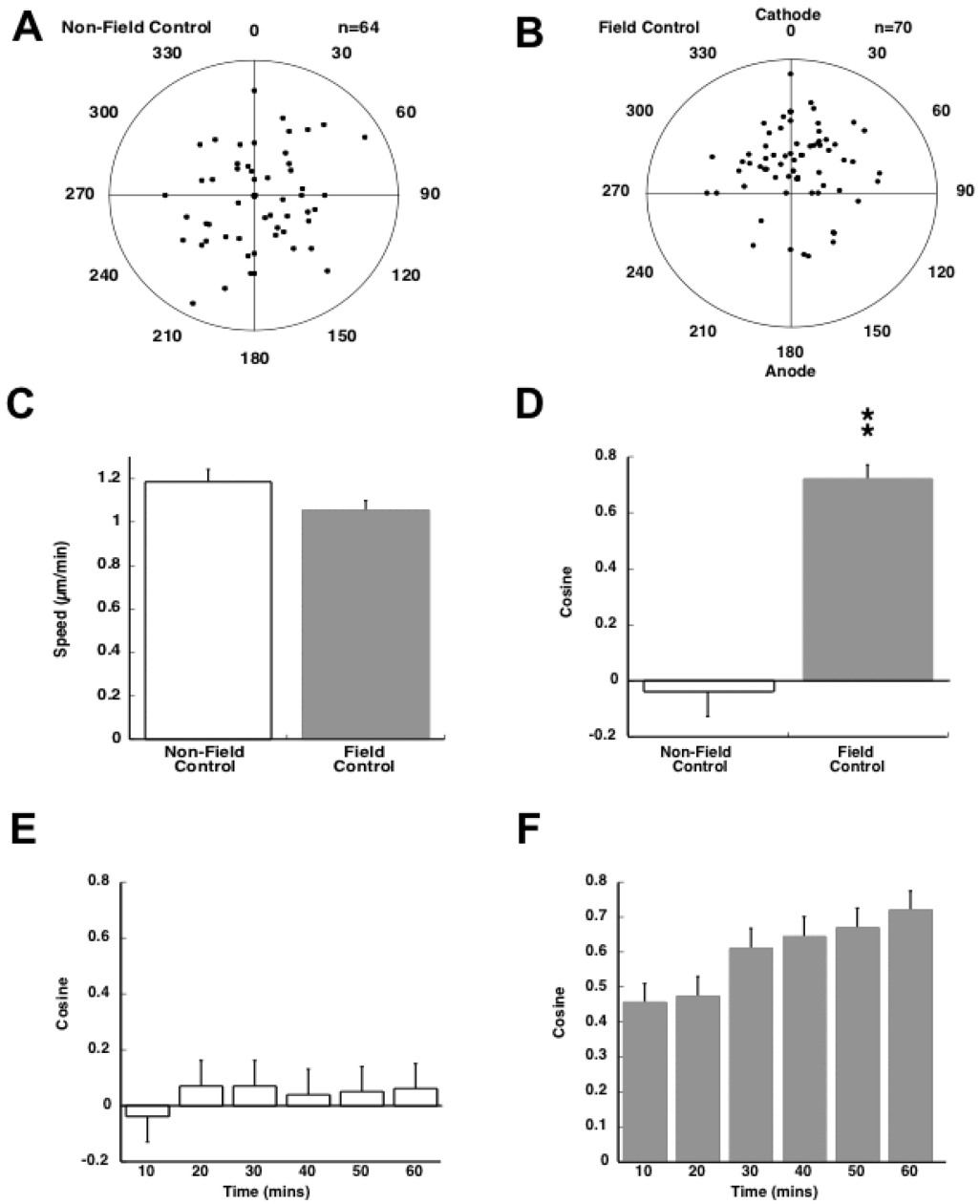
A
Non-Field Control
n=64
0
30
60
90
120
150
180
210
240
270
300
330
B
Field Control
Cathode
n=70
Anode
C
Speed (μm/min)
Non-Field Control
Field Control
D
Cosine
**
E
Cosine
Time (mins)
F
Cosine
Time (mins)

1

Figure 2

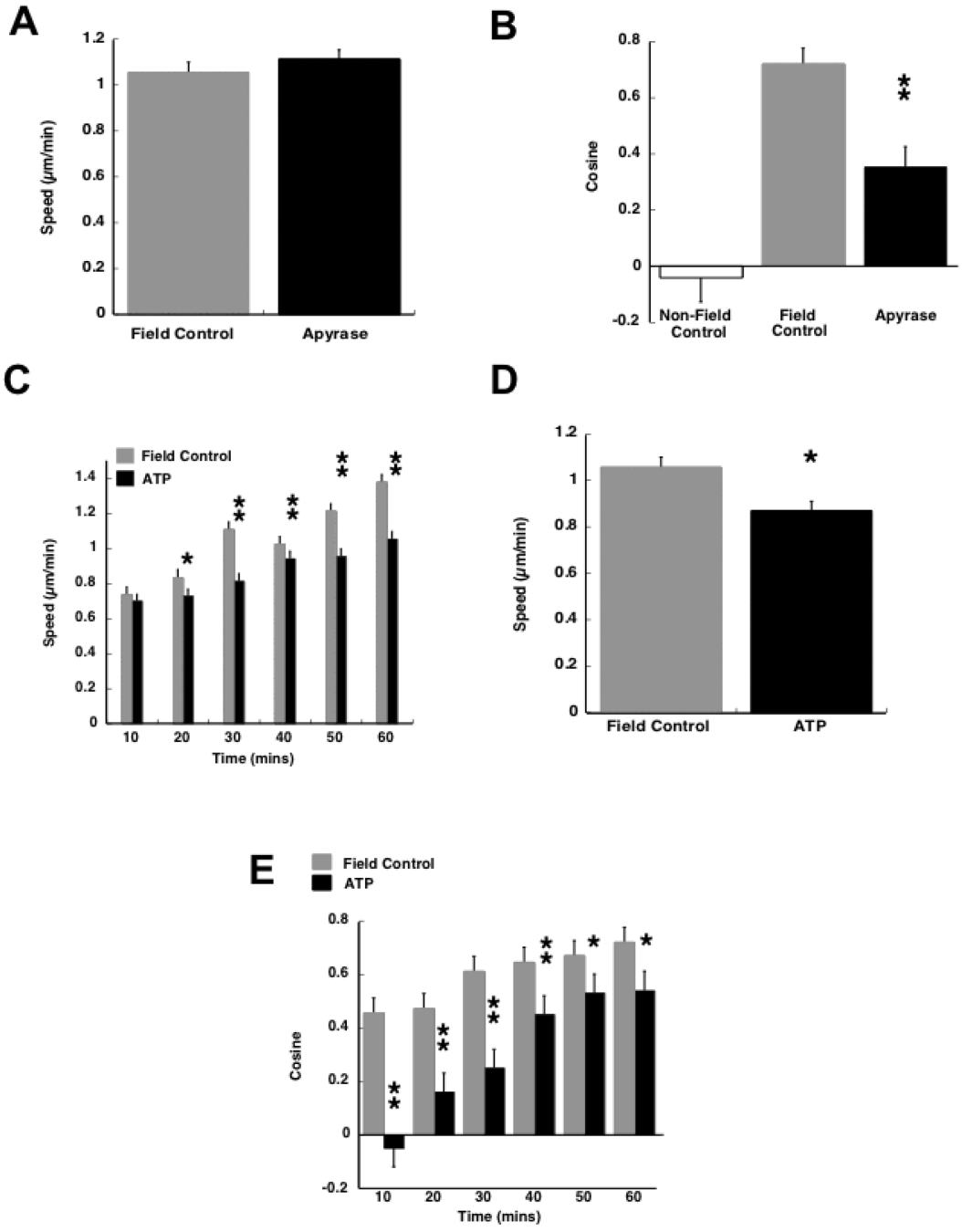
A
Speed (μm/min)
1.2
1
0.8
0.6
0.4
0.2
0
Field Control
Apyrase
B
Cosine
0.8
0.6
0.4
0.2
0
-0.2
Non-Field Control
Field Control
Apyrase
C
Field Control
ATP
Speed (μm/min)
1.4
1.2
1
0.8
0.6
0.4
0.2
0
10
20
30
40
50
60
Time (mins)
D
Speed (μm/min)
1.2
1
0.8
0.6
0.4
0.2
0
Field Control
ATP
E
Field Control
ATP
Cosine
0.8
0.6
0.4
0.2
0
-0.2
10
20
30
40
50
60
Time (mins)

1

Figure 3

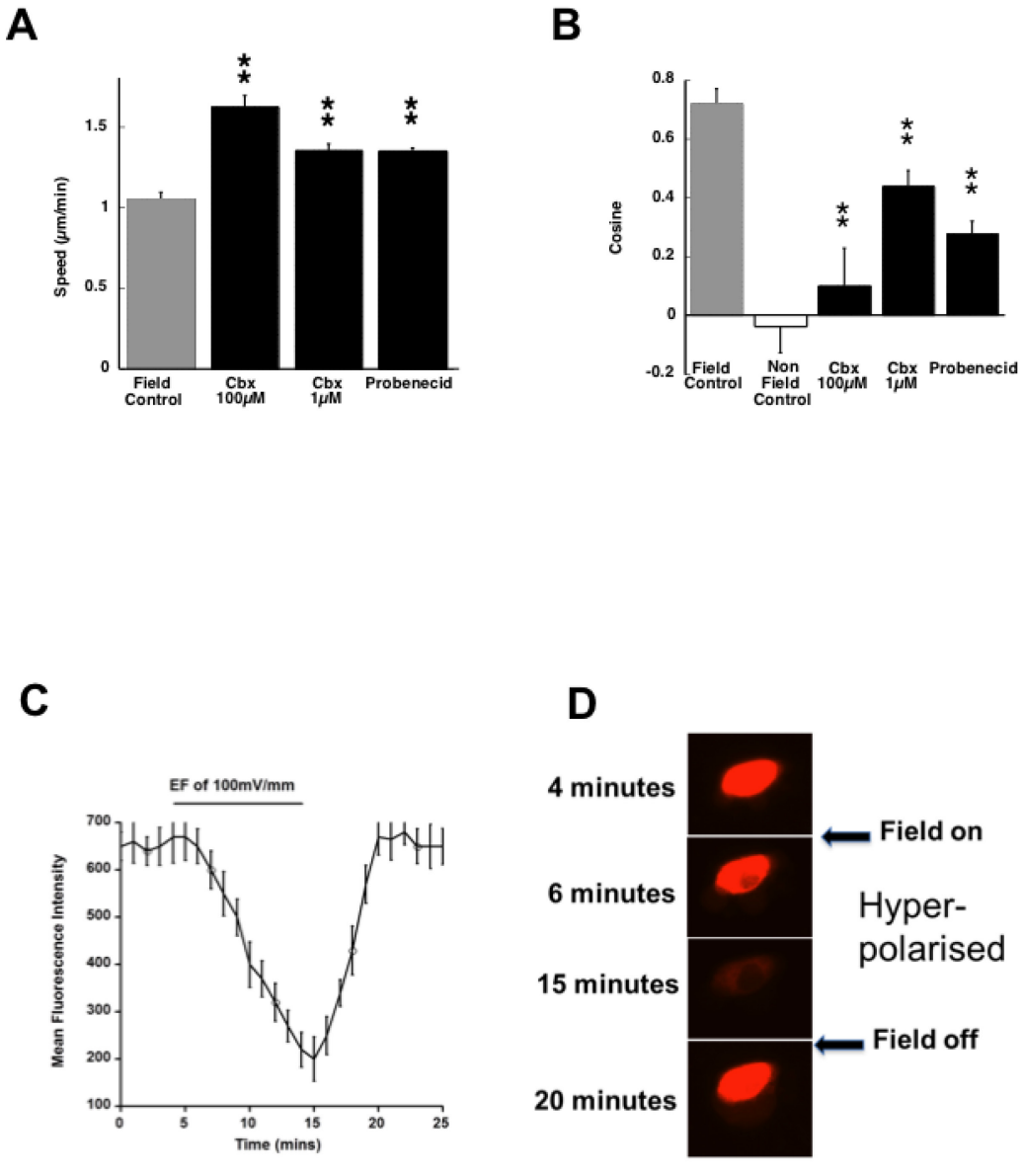
A
Speed (μm/min)
1.5
1
0.5
0
Field Control
Cbx 100μM
Cbx 1μM
Probenecid
B
Cosine
0.8
0.6
0.4
0.2
0
-0.2
Field Control
Non Field Control
Cbx 100μM
Cbx 1μM
Probenecid
C
EF of 100mV/mm
Mean Fluorescence Intensity
700
600
500
400
300
200
100
0
5
10
15
20
25
Time (mins)
D
4 minutes
6 minutes
15 minutes
20 minutes
Field on
Hyper-polarised
Field off

1

Figure 4

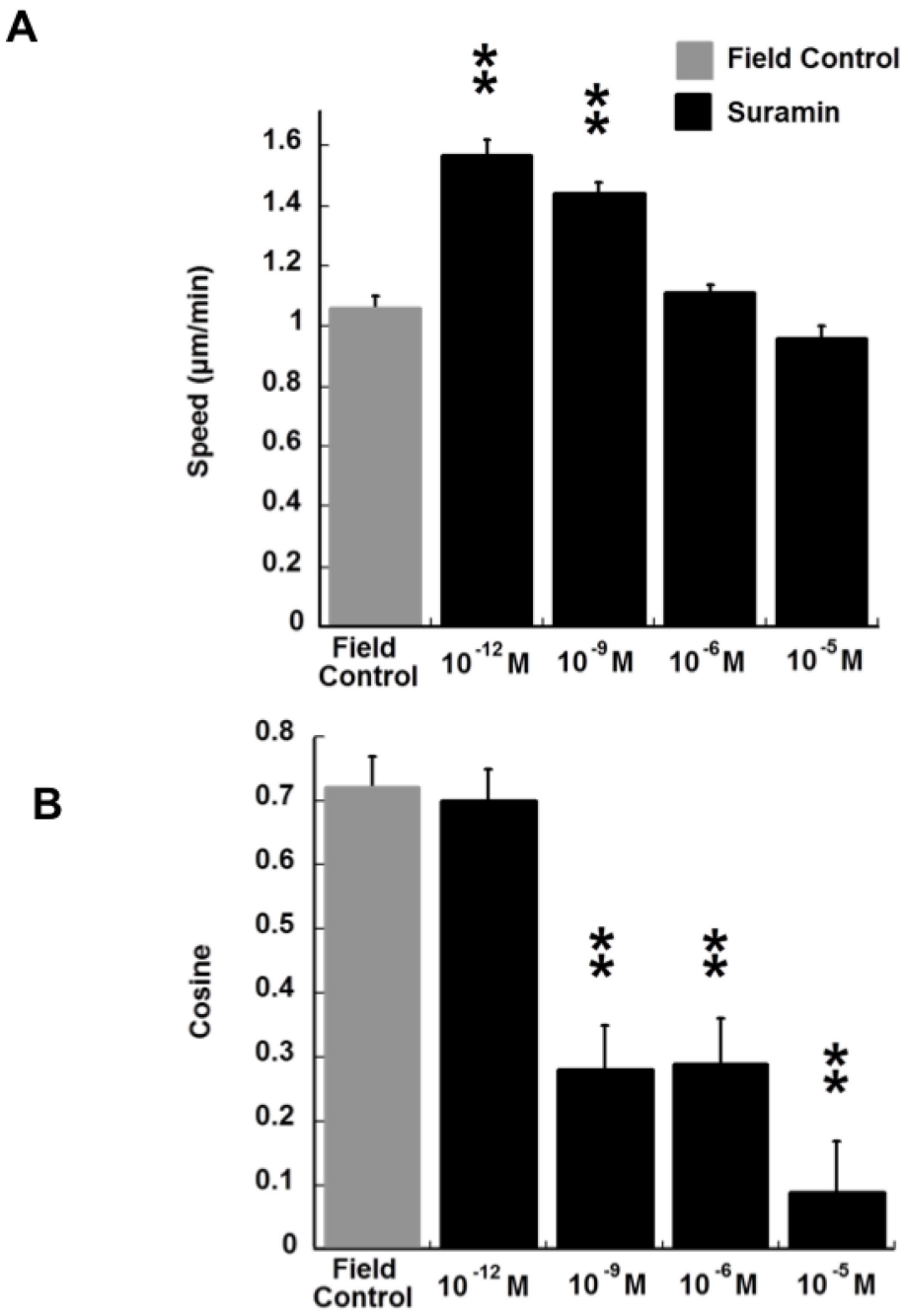
A
Field Control
Suramin
Speed (μm/min)
1.6
1.4
1.2
1
0.8
0.6
0.4
0.2
0
**
**
Field Control
10-12 M
10-9 M
10-6 M
10-5 M
B
Cosine
0.8
0.7
0.6
0.5
0.4
0.3
0.2
0.1
0
**
**
**
Field Control
10-12 M
10-9 M
10-6 M
10-5 M

1

Figure 5

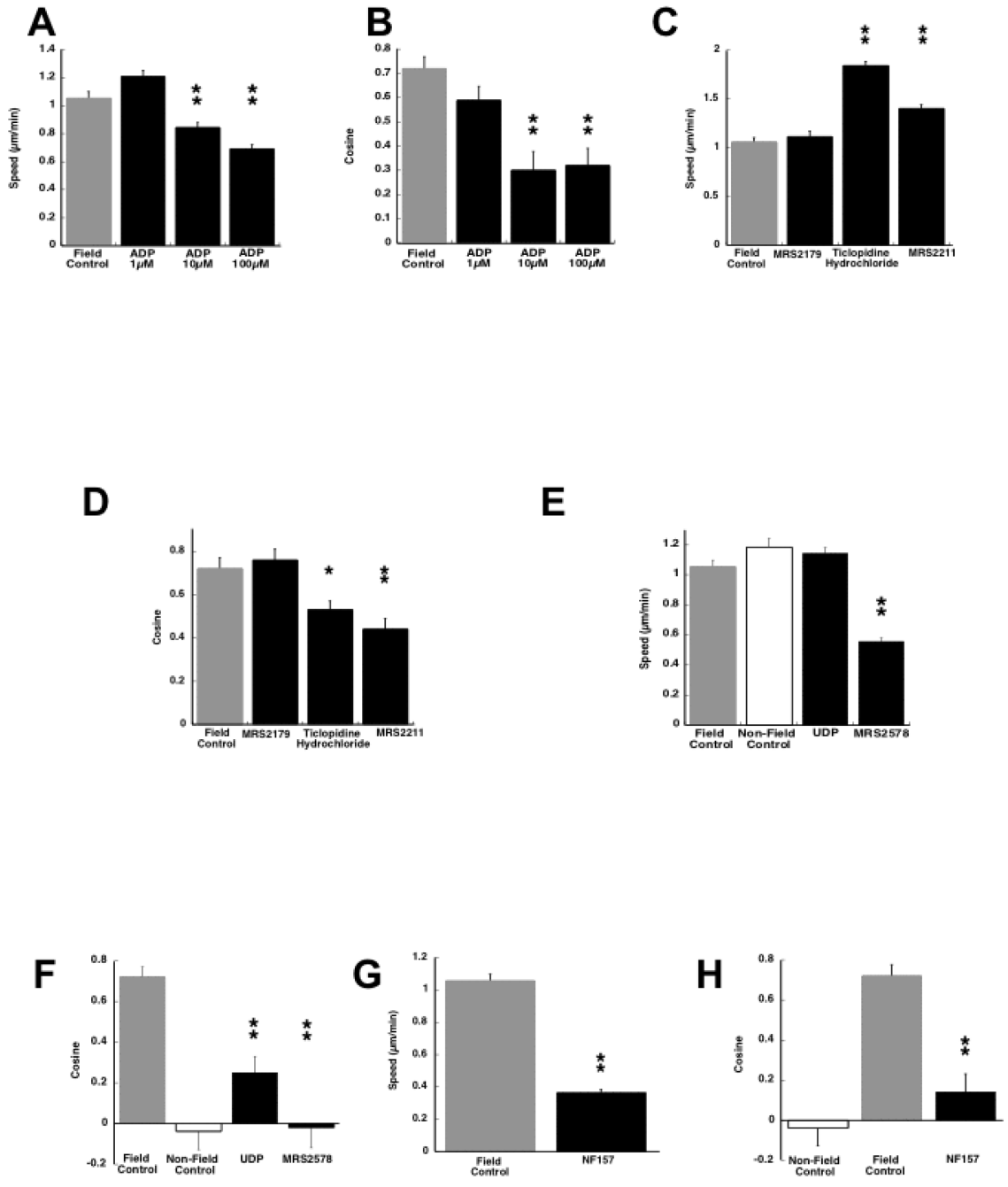
A
Speed (μm/min)
Field Control
ADP 1μM
ADP 10μM
ADP 100μM
B
Cosine
Field Control
ADP 1μM
ADP 10μM
ADP 100μM
C
Speed (μm/min)
Field Control
MRS2179
Ticlopidine Hydrochloride
MRS2211
D
Cosine
Field Control
MRS2179
Ticlopidine Hydrochloride
MRS2211
E
Speed (μm/min)
Field Control
Non-Field Control
UDP
MRS2578
F
Cosine
Field Control
Non-Field Control
UDP
MRS2578
G
Speed (μm/min)
Field Control
NF157
H
Cosine
Non-Field Control
Field Control
NF157

1

Figure 6

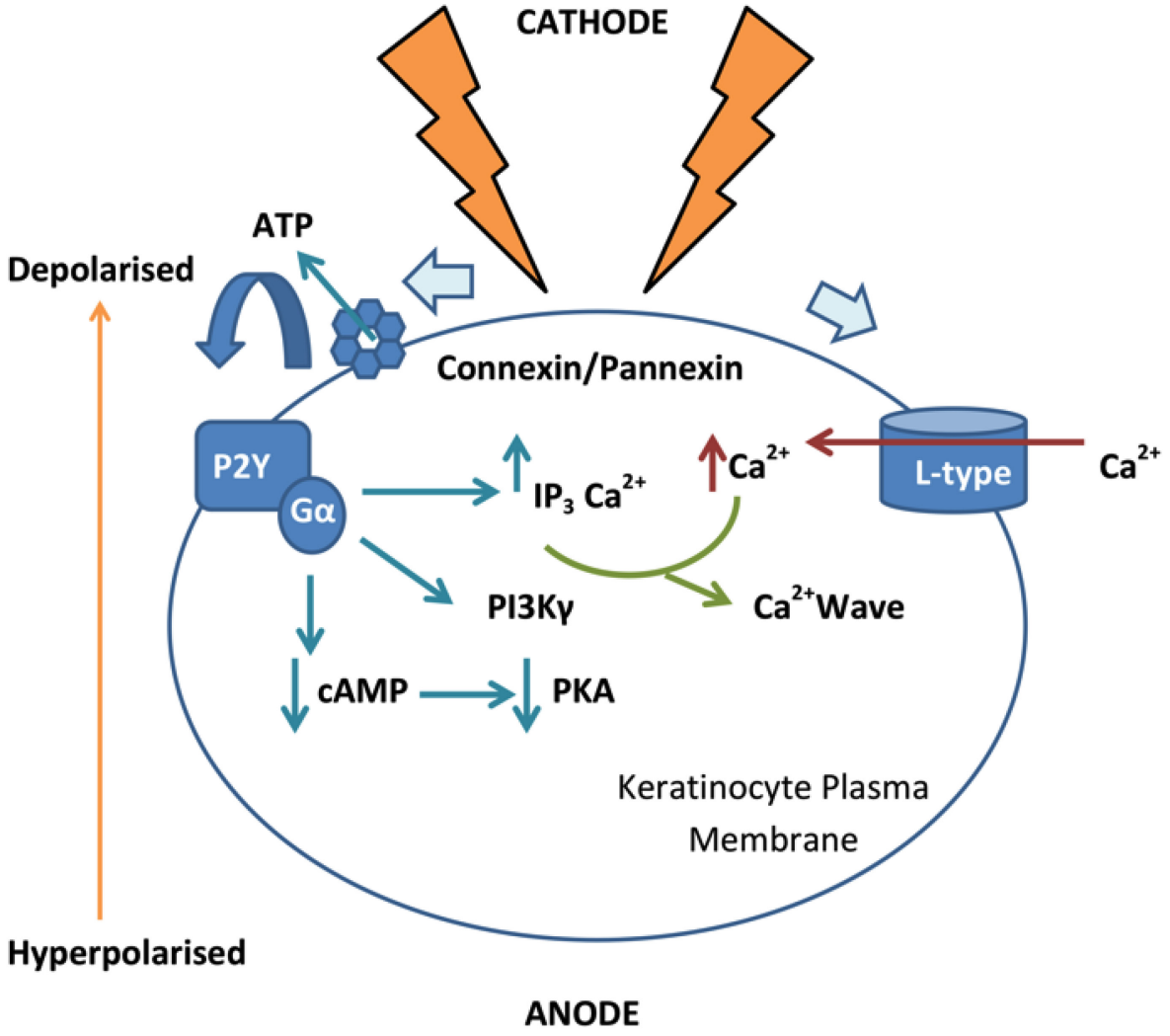
CATHODE
ATP
Depolarised
Connexin/Pannexin
P2Y
Gα
IP3 Ca2+
Ca2+
L-type
Ca2+
PI3Kγ
Ca2+Wave
cAMP
PKA
Keratinocyte Plasma Membrane
Hyperpolarised
ANODE

1